Advanced characterization of polyphenols from Myrciaria jaboticaba peel and lipid protection in in vitro gastrointestinal digestion

Adriana Gadioli Tarone, Pascale Goupy, Christian Ginies, Mario Roberto Marostica, Claire Dufour

HAL Id: hal-03295982
https://hal.inrae.fr/hal-03295982v1

1   **Advanced characterization of polyphenols from *Myrciaria jaboticaba* peel and**

2   **lipid protection in *in vitro* gastrointestinal digestion**

3

4   Adriana Gadioli Tarone[1], Pascale Goupy[2], Christian Ginies[2], Mario Roberto Marostica Junior[1],

5   Claire Dufour[2]*

6   [1]UNICAMP - University of Campinas, School of Food Engineering, LANUM; Rua Monteiro

7   Lobato, 80; Campinas-SP; CEP:13083-862; Brazil

8   [2]INRAE, Avignon University, UMR408 SQPOV, F-84000 Avignon, France

9   * Corresponding author.

10   E-mail address: claire.dufour@inrae.fr

11

12   **Abstract**

13   Ultrasound-assisted and solvent extractions led to similar levels in hydrolyzable tannins (10.3-6.0

14   mg/g), anthocyanins (7.8-10.2 mg/g) and flavonols (0.24-0.32 mg/g) for dried *Myrciaria jaboticaba*

15   peel (DJP). Ultrasound was efficient for the extraction of poorly soluble hydrolyzable tannins but

16   affected the stability of anthocyanins and flavonols. UPLC-DAD-MS^n allowed the identification of

17   44 hydrolyzable tannins as single and mixed hexosides bearing galloyl, HHDP and tergalloyl units.

18   Twelve mixed HHDP-galloylgluconic acids and tergalloylated hexosides were newly discovered in

19   this work. Acid hydrolysis of both ultrasonic extract and DJP yielded five major compounds, *i.e.*

20   gallic acid, ellagic acid, gallic acid-C-hexoside, valoneic acid dilactone and sanguisorbic acid

21   dilactone and pointed to higher contents in hydrolyzable tannins than by summing individual

22   polyphenols after UPLC. Last, cyanidin-3-*O*-glucoside and hydrolyzable tannins from the ultrasonic

23   extract inhibited lipid peroxidation of a Western type meal in *in vitro* digestion, suggesting a health

24   benefit for these jabuticaba polyphenols.

25

1. Introduction

Jabuticaba (*Myrciaria jaboticaba* (Vell.) O. Berg, also known as *Plinia cauliflora* (Mart.) Kausel), is a typical Brazilian berry from the *Myrtaceae* family. Fruits, presenting a dark violet peel and a white gelatinous pulp at maturity, are consumed *in natura* but also largely after processing. Because of its stiffness and astringent taste, the peel (up to 35% of the fruit weight) is not consumed leading to wastes rich in phenolic compounds, mainly anthocyanins, flavonols, and hydrolyzable tannins (ellagitannins, gallotannins) (Neves, Stringheta, Gomez-Alonso, & Hermosin-Gutierrez, 2018; Morales et al., 2016; Plaza et al., 2016; Pereira, Barbosa, da Silva, Ferri, & Santos 2017; Wu, Dastmalchi, Long, & Kennelly, 2012). These studies suggest the contribution of galloyl and hexahydroxydiphenoyl (HHDP) groups to jabuticaba hydrolyzable tannins although full identification and quantification of these tannins remain elusive owing to a large structural diversity and a lack of standards. Anthocyanins are present in high concentrations (0.14-3.2 g/100 g dry peel), mainly as cyanidin and delphinidin glucosides (Albuquerque et al., 2020; Quatrin et al., 2019; Plaza et al., 2016; Alezandro, Dube, Desjardins, Lajolo, & Genovese, 2013; Peixoto et al., 2016). Phenolic compounds appear to contribute to the *in vitro* antioxidant, antimicrobial, anti-proliferative and anti-inflammatory properties described for jabuticaba extracts (Albuquerque et al., 2020; Leite-Legatti et al., 2012). Moreover, jabuticaba fruit, tea and peel improve plasma lipid profile and insulin sensitivity, reduce lipid peroxidation in plasma and brain, and increase antioxidant enzyme activity in various organs of animal models for diabetes and obesity (Lenquiste et al., 2019; Alezandro, Granato & Genovese, 2013). A human study by Plaza et al. (2016) supported the preventive role of jabuticaba peel in metabolic diseases decreasing insulin and glucose levels. Acute and chronic human supplementations with anthocyanin-rich foods and extracts are clearly in favor of a health benefit in vascular protection (Fairlie-Jones et al., 2017). Of further interest, cardiometabolic risk biomarkers such as LDL-cholesterol, blood pressure or flow-mediated-dilation responded differently to ellagitannin-rich foods (pomegranate and nuts) and anthocyanin-containing products (berries and grape products) (Garcia-Conesa et al., 2018). Oxidative stress is a key factor

of inflammation and antioxidant phenolic compounds are expected to interfere with the production of reactive oxygen species even in locations such as the artery wall.

Only anthocyanin glucosides are bioavailable and the gastric mucosa was found to play an important role in absorption (Peixoto et al., 2016). Other anthocyanin glycosides and ellagitannins are not absorbed in the upper gastrointestinal tract and are further metabolized in the colon by the microbial flora. Ellagitannins mainly yield urolithins (Quatrin et al., 2020) while anthocyanins are cleaved to small phenolic acids such as protocatechuic acid and phloroglucinaldehyde (de Ferrars et al., 2014). The resulting microbial metabolites are partly deoxygenated and subjected to phase II metabolism resulting in a partial masking of residual hydroxyl groups. Bioavailable forms of anthocyanins and ellagitannins are thus less likely to play an antioxidant role in the circulation compared to their native forms.

As a matter of fact, the gastrointestinal tract has been proposed as a major site for diet-related oxidative stress and antioxidant activity of plant polyphenols (Gobert et al., 2014). Red meat iron, as provided by the Western diet, can trigger the oxidation of dietary polyunsaturated lipids leading to the formation of 4-hydroxyalkenals. These reactive lipid oxidation products are absorbable and further recovered in lipoproteins. LDL covalent modification is a key event in atherogenesis. Besides, the presence of cytotoxic and genotoxic 4-hydroxynonenal (4-HNE) in feces and plasma was correlated to the development of colonic preneoplastic lesions and atherosclerotic plaques in rodents fed with diets enriched in heme iron and polyunsaturated lipids. Interestingly, polyphenol-rich red wine and pomegranate extracts were found to decrease heme-induced luminal peroxidation and the promotion of colonic lesions (Bastide et al., 2017). On the other hand, both apple puree and extract inhibited the formation of 4-HNE in feces and plasma and largely reduced aortic plaque formation (Bolea et al., 2021).

Because anthocyanins display a large spectrum of coloring properties, they are nowadays widely used as natural food additives in dairy products and beverages. Ultrasound-assisted extraction of the jabuticaba peel and further extract stabilization by encapsulation are currently investigated to take

advantage of polyphenol nutritional and sensory properties (Tarone, da Silva, Cazarin & Marostica Junior, 2021). Besides, peel extracts were shown to display antioxidant and antimicrobial activities in sausages (Baldin et al., 2016).

The first objective of this work was to assess the efficiency of high-intensity ultrasound for polyphenol extraction from dried jabuticaba peel by comparison with solvent extraction using full structural elucidation and quantification by UPLC/DAD/ESI-MS^n. Next, the ultrasonic extract was compared to pure cyanidin-3-*O*-glucoside for its capacity to inhibit lipid oxidation in the *in vitro* gastrointestinal digestion of a Western type diet. Anthocyanin recovery was further evaluated.

2.   Materials and Methods

2.1.   Materials

Cyanidin-3-*O*-glucoside (C3G), gallic acid, ellagic acid and quercetin 3-*O*-glucoside were purchased from Extrasynthese (Genay, France). Methanol, acetonitrile, hexane and 2-propanol were HPLC-MS grade from Fisher Scientific (Illkirch, France); formic acid was HPLC-MS grade from Merck (Darmstadt, Germany). Ultrapure water (resistivity 18.2 MΩ/cm at 25 °C) was obtained with a Millipore OPak 2 (Millipore Corporation, Bedford, MA, USA).

Horse heart myoglobin (M1882, type II), pepsin from porcine gastric mucosa (P6887, 2829 U/mg according to Minekus et al. (2014)), porcine pancreatin (P7545, trypsin activity 2.8 U/mg according to Minekus et al. (2014)), porcine bile extract (B8631) and 2,4-dinitrophenylhydrazine (DNPH) were purchased from Sigma-Aldrich (Saint-Quentin Fallavier, France). 4-Hydroxy-2-nonenal and 4-hydroxy-2-nonenal-D3 were purchased from Bertin Pharma (Montigny le Bretonneux, France). Commercial sunflower oil, from Auchan (lot No. A07611), was stored at –20 °C after purchase. L-α-phosphatidylcholine from dried egg yolk (PL) (P3556) was from Fluka (Buchs, Switzerland). Oil and PL compositions are detailed in the Supplementary Material.

2.2.   Jabuticaba peel extracts

2.2.1. Jabuticaba peel processing

Jabuticaba (*Myrciaria jaboticaba* (Vell.) O. Berg) fruits were kindly donated by "Indústria e Comércio Lagoa Branca Ltda", located at Boa Vista II Farm, in White House city (São Paulo, Brazil) under the authorization of the Brazilian Management System of National Genetic Heritage and Traditional Associated Knowledge (#A72354F) (August 2016). The species used in this work was assessed by comparison with species deposited in the herbarium of the Agronomic Institute of Campinas, Santa Elisa farm, numbers 48093 and 48094.Twenty kg of fresh fruits were washed, manually peeled and the peel was dried in a stove with air circulation (Marconi, Piracicaba, SP, Brazil) at 40 °C for 72 h until constant weight. The dried peel (ca. 1 kg) was transformed in a fine powder with an electrical mill (Marconi, MA 630/1, Piracicaba, SP, Brazil) and sifted (mash 20). The dried jabuticaba peel powder (DJPP) was packed in plastic bags under vacuum and stored at - 20 °C until use.

2.2.2. Dried jabuticaba peel extraction by ultrasound (DJP-US)

DJPP prepared as above (1 g) was added into a falcon with 25 mL of 50% ethanol in ultrapure water (v/v) and sonicated using a 13-mm ultrasonic probe (Unique, Desruptor, 800 W, 19 kHz, Indaiatuba, Brazil) at an ultrasound intensity of 3.7 W/cm^2 for 3 min. The probe contact height within the dispersion was 40 mm and an ice bath was used (temp. < 35 ºC). The solvent was removed in vacuum at 37 °C. The extraction was made in triplicate. The dry residues were reconstituted in the same volume of ultrapure water before freeze-drying and storage at - 20 °C.

2.2.3. Dried jabuticaba peel extraction by a conventional solvent method (DJP-CM)

In a 2 mL microtube with conical bottom, 100 mg (for analysis of phenolic compounds) or 10 mg (for anthocyanin analysis) of DJPP were placed with balls of zirconium and 1.5 mL of extraction solvent (70% ethanol in ultrapure water (v/v) containing 1% of formic acid). After

6

135   shaking at 1200 rpm for 45 s in a 1600 MiniG® SPEX Sample Prep (New Jersey, USA), the

136   microtube was centrifuged at 16000 g and 4 °C for 5 min. The supernatant was collected and the

137   residue was extracted again twice in the same conditions. Supernatants were pooled, the solvent was

138   evaporated in vacuum at 37 °C and the sample was stored at - 20 °C until analysis. The extraction

139   was made in triplicate.

140

141   *2.2.4. Hydrolysis of phenolic compounds*

142   The hydrolysis of the phenolic extracts was conducted according to Garcia-Villalba et al.

143   (2015) with some modifications. DJP-US or DJPP (100 mg) was put into a glass tube with 3.34 mL

144   of ultrapure water and 1.66 mL of 37% HCl. The tube was vortexed for 1 min and incubated at 90

145   °C for 24 h. After cooling to room temperature, the pH was adjusted to 2.5 with 5 M NaOH and the

146   volume adjusted to 6 mL with water in a graduated syringe. After centrifugation (5 min, 16000 g

147   and 4 °C), the supernatant was recovered and filtered through a Minisart RC4 filter before injection

148   onto UPLC/DAD/ESI-MS[n]. The residual pellet was vortexed twice with 1 mL of DMSO/MeOH

149   (50:50, v/v) for 2 min and centrifuged as above. The mixed supernatants were filtered through a

150   Minisart RC4 filter before analysis. All samples were prepared in triplicate.

151

152   **2.3 Identification and quantification of phenolic compounds and anthocyanins**

153   Freshly reconstituted solutions of DJP-US and DJP-CM extracts were prepared in 98 vol. of

154   1% formic acid in ultrapure water (v/v) and 2 vol. of 1% formic acid in acetonitrile (v/v) at

155   concentrations of 100 mg/mL and 1 mg/mL for UPLC/DAD/ESI-MS[n] analysis of phenolic

156   compounds and anthocyanins, respectively. Separation and mass conditions are detailed in the

157   Supplementary Material.

158   The quantification was performed using 5 to 10 point-calibration curves with C3G,

159   quercetin-3-*O*-glucoside, gallic acid and ellagic acid. All the standards were prepared in methanol

160   except C3G in methanol acidified with 0.1% HCl (v/v). Gallic acid was quantified with its own

standard and gallic acid derivatives were quantified as gallic acid equivalent at 280 nm; ellagic acid was quantified with its own standard and ellagic acid derivatives as ellagic acid equivalent at 370 nm; quercetin derivatives and myricetin derivatives as quercetin-3-O-glucoside equivalent at 370 nm, and anthocyanins as C3G equivalent at 520 nm.

2.4 Simulated static *in vitro* gastrointestinal digestion

2.4.1   Preparation of the simulated digestion fluids and antioxidants

The simulated gastric (SGF) and intestinal (SIF) fluids were made up as described in Minekus et al. (2014). Enzymes were prepared prior to use. Porcine pepsin was prepared as an 8.08 mg/mL solution in SGF for a final concentration in the gastric phase of 1000 U/mL. Porcine pancreatin was prepared as a 94 mg/mL solution in SIF for a final concentration in the intestinal phase of 100 U trypsin/mL. The porcine bile extract was prepared as a 20.85 mg/mL solution in SIF for a final concentration of 5 mg/mL (ca. 10 mM) in bile salts. $CaCl_2$ $(H_2O)_2$ (0.1 mM), HCl (0.1 M) and NaOH (0.25 M) were prepared in ultrapure water. DJP-US (1 mg or 5 mg) was dissolved prior to use in 1 mL of SGF to bring respectively 14.88 µg (US-1) or 74.4 µg (US-5) of total anthocyanins with 89% of C3G and 11% of delphinidin-3-O-glucoside (D3G). C3G-1 and C3G-5 were prepared by adding 21 and 104 µL of C3G at 0.859 mg/mL in methanol acidified with 0.1% HCl (v/v) to 1979 and 1896 µL of SGF, respectively.

2.4.2   Preparation of oil-in water emulsions

The physical state of lipids during digestion was simulated by a 12.5% oil-in-water emulsion stabilized by egg yolk L-α-phosphatidylcholine (PL). In a 60 mL short-necked glass bottle, 5 g of sunflower oil were added to 100 mg of PL previously dispersed in 35 mL of SGF under magnetic stirring. The mixed oil and aqueous phases were then homogenized using a rotor stator homogenizer (Silent Crusher M-01, Heidolph) at 24000 rpm for 2 min. The resulting coarse

186 emulsion was sonicated on ice for 8 periods of 30 s with rest intervals of 30 s and an amplitude of

187 60% (Q700, QSonica, 20 kHz). See Suppl. Material for emulsion characterization.

188

189 *2.4.3 Lipid oxidation in in vitro gastrointestinal digestion*

190 The physicochemical conditions for *in vitro* static gastrointestinal digestion were from

191 Minekus et al. (2014) with slight modifications. First, 12 mL of the fine emulsion were placed in a

192 50 mL round-bottom flask containing a magnetic stirrer. For the gastric phase, 1 mL of pepsin, 50

193 µL of 0.1 mM $CaCl_2$, 1 mL of antioxidant solution (US-1, US-5, C3G-1 or C3G-5) or 1 mL of SGF

194 for the blank were added. If necessary, the pH was adjusted to 5 with 0.1 M HCl or 0.25 M NaOH.

195 The first sample was collected (G0). Lipid oxidation was initiated by adding 2.5 mL of 200 µM

196 $MbFe^{III}$ prepared in SGF (using ε =7700 $L.mol^{-1}.cm^{-1}$ at 525 nm (Bolea et al., 2019) to reach a final

197 concentration of 30 µM. Bottom flasks were protected by punched parafilm and incubated in an

198 oven at 37 °C under stirring at 280 rpm during 60 min with sampling at 30 and 60 min. After 60

199 min, the pH was adjusted to 3 with 0.1 M HCl and the digestion was carried on another 60 min

200 (sampling at 90 and 120 min). After 2 hours of gastric digestion, pancreatin (6.5 mL), bile (6 mL),

201 and $CaCl_2$ (75 µl) were then added to simulate the intestinal phase. pH was adjusted to 6.5 with 0.25

202 M NaOH and sampling continued for the next 2 h. Experiments were run at least in triplicate.

203

204 *2.4.4 Determination of lipid oxidation products*

205 Digesta samples (200 µL) were diluted in a microtube with 1000 µL of a 2-propanol/hexane

206 (2:3, v/v) mixture, vortexed and centrifuged (10 min, 16 200 *g*, 4 °C). The upper hexane phase (ca.

207 600 µL) was collected and 1200 µL of hexane were added to the lower phase, vortexed and

208 centrifuged as above. Pooled hexane phases were evaporated under nitrogen and taken up in 2 mL

209 of 2-propanol to yield extract S1. S1 was immediately used for measurement of conjugated dienes

210 (CD) then stored at -20 °C until the determination of 4-hydroxy-2-nonenal (4-HNE).

211

212   2.4.4.1 <u>Measurement of lipid-derived conjugated dienes (CD)</u>

213   After further dilution of S1 (300 µL) in 2-propanol (1700 µL), the concentration in CD was

214   determined by measuring the absorbance at 234 nm (HP 8453 diode-array spectrometer) using a

215   molar absorption coefficient of 27 000 $M^{-1}cm^{-1}$ for conjugated linoleyl hydroperoxides.

216

217   2.4.4.2 <u>Measurement of 4-hydroxy-2-nonenal</u>

218   The secondary lipid oxidation product 4-HNE was derivatized with DNPH before

219   quantification in the MRM mode in HPLC-MS (See Supplementary Material).

220

221   *2.4.5   Determination of anthocyanin bioaccessibility*

222   Anthocyanin bioaccessibility was defined as the content in free C3G and D3G in the aqueous

223   phase of the digesta. Digesta samples (600 µL) were collected and placed in a microtube with 50 or

224   75 µL of 0.1 M HCl for gastric and intestinal samples, respectively. After centrifugation (16 200 *g*

225   for 10 min at 4 °C), the aqueous phase was removed via syringe, filtered (Phenex RC 0.45 µm) and

226   stored at - 20 °C until anthocyanin analysis by UPLC/DAD/ESI-MS^n as described in section 2.3.

227

228   **2.5   Statistical analyses**

229   All the results are expressed as mean ± standard deviation (SD). One-way analysis of variance

230   (ANOVA) with repeated measures was performed to test the effect of variation factors. If

231   significant effects were found at a 95% confidence level, ANOVA was followed by a Tukey-

232   Kramer post hoc test to identify differences among groups (XLStat software (2020), Addinsoft,

233   Paris, France).

234

3. Results and discussion

3.1. Profile and content in phenolic compounds and anthocyanins of dried jabuticaba peel by UPLC/DAD/ESI-MS^n analyses

In order to assess the effect of ultrasound on polyphenol extraction, the extracts produced by ultrasound-assisted extraction and conventional solvent extraction of dried jabuticaba peel were compared through their profiles in phenolic compounds and anthocyanins (Fig. 1 & Fig. S1 in Suppl. Mat.). For both extracts, the same 58 phenolic compounds were tentatively identified (Table 1). Maximum absorption wavelength, molecular ion and fragmentation pattern in MS were used in the absence of standards for structure assessment.

3.1.1. Hydrolyzable tannins

Hydrolyzable tannins are polyesters between a sugar moiety and hydroxylated benzoic acid derivatives. In the DJP-US and DJP-CM extracts, gallic acid and ellagic acid were the main contributors. Gallic acid was not found free but esterified by a hexose unit which could be glucose according to Pereira et al. (2017). Galloylhexose (**1**) displays a parent ion at *m/z* 331 with major fragment ions at *m/z* 271 and 169, which are typical of galloylglucose fragmentation (Quatrin et al., 2019). Di- (**4**, **22**; *m/z* 483), tri- (**34**; *m/z* 635), tetra- (**44**, **46**; *m/z* 787) and pentagalloylhexoses (**50**; *m/z* 939) were recovered as several isomers, as found in jabuticaba (Quatrin et al., 2019) and in pomegranate (Garcia-Villalba et al., 2015).

Ellagic acid was found free (**42**; *m/z* 301) and bound to a hexose moiety (Pereira et al., 2017; Plaza et al., 2016; Morales et al., 2016; Fischer, Carle, & Kammerer, 2011). Ellagic acid pentoside (**39**) displays a parent ion at *m/z* 433 and a major fragment at *m/z* 301 indicating the loss of a pentose unit. The hexahydroxydiphenoyl (HHDP) group related to ellagic acid appears in five isomeric di-HHDP-hexosides (**6**, **9**, **10**, **17, 40**). Two of them, **10** and **17**, could be quantified. They display a parent ion at *m/z* 783 and major fragments at *m/z* 481 and 301 indicating the loss of a HHDP group except **40** which gave a dehydrated form first (*m/z* 765). Previous studies (Quatrin et

261   al., 2019; Plaza et al., 2016; Wu et al., 2012) reported 2 isomers in jabuticaba peel while Silva et al.

262   (2016) isolated pedunculagin from jabuticaba seed and Garcia-Villalba et al. (2015) found one

263   isomer in pomegranate.

264   A larger group of hydrolyzable tannins is constituted by mixed esters containing both galloyl

265   and HHDP groups. Quantified HHDP-galloylhexose isomers (**2**, **5, 16**, **25**) display a parent ion at

266   *m/z* 633 and a major fragment ion at *m/z* 301 indicating the loss of HHDP. HHDP-digalloylhexose

267   isomers (**21**, **29**, **37**) were evidenced as previously described in *Myrciaria* species (Quatrin et al.,

268   2019; Plaza et al., 2016; Fracassetti, Costa, Moulay, & Tomas-Barberan, 2013). They present a

269   parent ion at *m/z* 785 and fragment ions at *m/z* 633 and 483 resulting from the loss of a galloyl or a

270   HHDP group. They were all quantified. For di-HHDP-galloylhexoses (**26**, **27**, **36**), with a parent ion

271   at *m/z* 935, two different fragmentation patterns are observed. Isomer **26** fragments to yield a major

272   ion at *m/z* 917 (-H$_2$O) while the two others yielded *m/z* 633 in agreement with the loss of a HHDP

273   group. Isomeric casuarictin, stachyurin, potentillin and casuarinin have been tentatively identified in

274   jabuticaba (Quatrin et al., 2019; Pereira et al., 2017; Plaza et al., 2016), camu-camu (Fracassetti et

275   al., 2013) and pomegranate (Fischer et al., 2011; Garcia-Villalba, et al., 2015). Casuarictin was

276   formerly identified by NMR in *Myrciaria cauliflora* by Pereira et al. (2017). Fast elution, close

277   retention times but different fragmentation schemes are observed for **26** and **27** suggesting that

278   these compounds could be casuarinin and casuarictin (Plaza et al., 2016). Di-HHDP-

279   digalloylhexose (**55**) displays a parent ion at *m/z* 1087 with a major fragment ion at *m/z* 917 (loss of

280   gallic acid) as well as a fragment ion at *m/z* 749 (loss of hexahydroxydiphenic acid). This

281   compound is tentatively reported for the first time for the jabuticaba species. Finally, HHDP-

282   trigalloylhexose (**41**) is characterized by a parent ion at *m/z* 937 and displays losses of gallic acid

283   (*m/z* 767), HHDP (*m/z* 635), gallic acid + HHDP (*m/z* 465) and formation of ellagic acid (*m/z* 301)

284   (Plaza et al., 2016; Fracassetti et al., 2013). They were all quantified except **55**.

285   HHDP-galloylgluconic acid (**3**), HHDP-digalloylgluconic acids (**8**, **12**) and di-HHDP-

286   galloylgluconic acids (**13**, **18**, **19** and **31**) are tentatively reported for the first time in the jabuticaba

12

species although they were previously described Tanaka et al. (1992) in pomegranate and *Lagerstroemia speciosa*. The parent ions at m/z 649, 801 and 951 differ by 16 amu from those found for HHDP-galloylhexose (m/z 633), HHDP-digalloylhexose (m/z 785) and di-HHDP-galloylhexose (m/z 935). Major fragment ions at m/z 605, 757 and 907 indicate the loss of CO_2 which is in agreement with the presence of a carboxylic acid function. HHDP (m/z 301) could be observed in MS^3 for **3** while the loss of HHDP was observed in the MS^2 fragmentations of **13**, **18**, **19** and **31** with m/z 605 resulting from the major fragment at m/z 907. They proved to be in smaller amounts compared to related hexose derivatives. Additionally, the fragmentation of compound **31**, proposed to be di-HHDP-galloylgluconic acid, totally differs from that reported for DHHDP-HHDP-galloylglucose in pomegranate (Calani et al., 2013).

Isomeric nonahydroxyterphenic acid dilactones (**14** and **30**) were detected as previously found in jabuticaba (Wu et al., 2012) and camu-camu (Fracassetti et al., 2013). They presented a parent ion at m/z 469 and a major fragment ion at m/z 425 (loss of CO_2) and differed remarkably by their retention times. Compound **14** was not further fragmented and it was thus assigned as tergallic acid dilactone owing to likely strong C-C bonds between gallic acid units. Additional fragmentation for **30** revealed fragments at m/z 407, 301 and 167. Fragment m/z 301 corresponds to ellagic acid and is in favor of an additional labile ether linkage between 2 aromatic units, as found for valoneic acid dilactone in pomegranate (Garcia-Villalba et al., 2015). Two compounds (**20** and **23),** in trace amounts, presented a parent ion at m/z 631 and a major fragment ion at m/z 451. The loss of 180 amu suggests the presence of a hexose moiety linked through a C- or O-glycosidic linkage to a tergalloyl group as found in jabuticaba (Quatrin et al., 2019) and in hydrolyzed pomegranate (García-Villalba et al., 2015). Pereira et al. (2017) identified 4,6-*O*-tergalloyl-D-glucose (Cauliflorin) by NMR in jabuticaba.

Six compounds with a parent ion at m/z 933 were identified although only 3 of them could be quantified. Fragment ions at m/z 451 and 631 are observed for four compounds (**15**, **33**, **38** and **52**) corresponding respectively to the tergalloyl group and the loss of HHDP from the parent ion.

313   This fragmentation pathway is consistent with structures such as vescalagin, castalagin, and α- or β-

314   alnusiins as reported in jabuticaba (Albuquerque et al., 2020; Quatrin et al., 2019). According to

315   Pereira et al. (2017) who secured by NMR experiment the structures of two these compounds,

316   vescalagin was only present in peel of *Myrciaria cauliflora* whereas vescalagin and castalagin were

317   both present in seeds and pulp. The two other compounds (**7**, **11**) eluted faster and display common

318   fragment ions at *m/z* 915 (- H_2O), 613 and 569, as observed for vescalagin and castalagin standards

319   (Tavares et al., 2016). Standards are thus required for the unequivocal attribution of these different

320   HHDP-tergalloylhexoses.

321   High-molecular weight compounds likely bearing a tergalloyl or a gallagyl group appeared

322   in trace amounts. They are reported for the first time in the jabuticaba species. Isomers **51** and **57**

323   display *m/z* at 1085 and 542, corresponding to singly and doubly charged ions, respectively, and a

324   fragment ion at *m/z* 633 which could be HHDP-galloylhexose. Isomers **53** and **56** displayed *m/z* at

325   1083 and 541 (doubly charged ion) and yielded *m/z* 631 upon fragmentation as found for

326   tergalloylhexose. It is worth noting that HHDP-galloyltergalloylhexose (MW 1086) exhibits the

327   same molecular weight as digalloylgallagylhexose and ditergalloylhexose (MW 1084) as HHDP-

328   digallagylhexose. However, only dilactones of valoneic acid and sanguisorbic acid (tergalloyl

329   derivatives) were quantified after acid hydrolysis and no gallagic acid dilactone could be recovered.

330   Hydrolyzable tannins **51**, **53**, **56** and **57** are thus clearly tergalloyl derivatives.

331

332   *3.1.2. Anthocyanins*

333   Two main anthocyanins, delphinidin-3-*O*-glucoside (D3G) and cyanidin-3-*O*-glucoside

334   (C3G) were identified, as described before in the jabuticaba peel (Figure 1B). D3G (**24**) displayed a

335   parent ion in the positive mode at *m/z* 465 with a major fragment ion at *m/z* 303 (loss of a hexose

336   moiety) (Plaza et al., 2016; Mena et al., 2012). C3G (**28**) ([M]$^{+}$ at *m/z* 449 and 287 in MS^2) was

337   identified by comparison with the standard compound. Minor pelargonidin-*O*-hexoside (**32,** [M]$^{+}$ at

338　*m/z* 433 and 271 in MS^2) and peonidin-*O*-hexoside (**35,** [M]$^+$ at *m/z* 463 and 301 in MS^2) were also

339　identified as previously in jabuticaba peel by Quatrin et al. (2019).

340

341　*3.1.3　　　Flavonols*

342　　　　Myricetin deoxyhexoside (**43**; *m/z* 463), quercetin hexosides (**45**, **47**; *m/z* 463) and quercetin

343　deoxyhexoside (**54**; *m/z* 447) display daughter ions at *m/z* 317 or 301, allowing to assign their

344　aglycone part (Figure 1C). For quercetin pentosides (**48**, **49**), their parent and fragment ions at *m/z*

345　433 and *m/z* 301 as well as their maximal absorption in the range 350-360 nm were not sufficient to

346　discriminate them from ellagic acid pentoside. However, they yielded in MS^n subsequent

347　fragmentation at *m/z* 273, 257, 179 and 151 which are typical of the benzopyrane moiety of

348　flavonols as evidenced for quercetin (**58**) (Neves et al., 2018)

349

350　*3.1.4　Others*

351　　　　No caffeoylquinic acids and flavan-3-ols ((epi)catechin, type-B procyanidin dimers,

352　(epi)catechin gallate, gallo(epi)catechin) could be evidenced in jabuticaba peel by search of their

353　parent ions. Thioacidolysis was additionally conducted on both peel extract and peel powder

354　indicating the absence of flavan-3-ol oligomers in these materials.

355

356　*3.1.5　Polyphenol quantification by UPLC/DAD*

357　　　　Quantification was possible for 32 and 27 compounds out of the 58 tentatively assigned for

358　the DJP-US and DJP-CM extracts, respectively (Table 2).

359　Gallic acid derivatives are the largest class of compounds found for both extracts. They comprise

360　single and mixed esters containing at least a galloyl or HHDP group. The DJP-US extract presented

361　the highest amount in gallic acid derivatives (9.2 ± 0.3 mg/g DJP), differing statistically from the

362　DJP-CM extract (4.9 ± 0.7 mg/g DJP). Contents between 3.5 and 8.2 mg/g DJP were previously

reported using different extraction methods and standards (Albuquerque et al., 2020; Quatrin et al., 2019; Plaza et al., 2016).

Similar levels in ellagic acid were quantified in both DJP-US and DJP-CM extracts (1.1 mg/g DJP) and these contents are in the same range as those found by Inada et al. (2015) (1.8 mg/g DJP), Plaza et al. (2016) (1.4 mg/g DJP) and Quatrin et al. (2019) (0.5 mg/g DJP) although without ellagic acid as standard for the latter two groups.

Anthocyanins, quantified as both C3G and D3G, are the second most abundant group. Contents in anthocyanins were found to be significantly lower for the DJP-US extract (7.8 ± 0.1 mg/g DJP) than for the DJP-CM extract (10.2 ± 1.2 mg/g DJP). Plaza et al. (2016) and Albuquerque et al. (2020) found higher amounts of anthocyanin derivatives (32.2 and 24.5 mg/g DJP, respectively) while Quatrin et al. (2019), Peixoto et al. (2016) and Alezandro, Dube et al. (2013) found relatively similar or lower amounts (11.5, 1.7, and 3.5 mg/g DJP).

Additionally, the DJP-CM extract presented a statistically higher level of flavonol derivatives (0.32 ± 0.02 mg/g DJP) than the DJP-US extract (0.24 ± 0.01 mg/g DJP). Both Quatrin et al. (2019) and Plaza et al. (2016) found similar amounts (0.6 mg/g DJP) with solvent and pressurized hot water extractions. Finally, our work did not reveal any differences for the overall contents in phenolic compounds whatever the extraction method used. Quantification differences between classes can be explained by the behavior of specific polyphenols towards ultrasound. The acoustic cavitation produced by ultrasound promotes a very efficient cell wall disruption. This may have considerably increased the transfer of galloyl, HHDP and tergalloyl hydrophobic esters to the liquid phase. However, this process promotes the creation of shear forces that generate critical temperature and pressure, locally generating hydroxyl radicals which cause the degradation of sensitive compounds such as anthocyanins and flavonols (Wang, Cheng, Ma, & Jia, 2020).

3.2 Acid hydrolysis of DJP and DJP-US extract

Acid hydrolysis of the dried jabuticaba peel and ultrasonic extract was conducted to release the phenolic depsides present as *O*-hexosides. Because of the low water solubility of the released phenolic compounds, an additional step of pellet washing by MeOH/DMSO (1:1) was performed as proposed by Garcia-Villalba et al. (2015). Identification and quantification of the compounds after acid hydrolysis are presented in Table 3 while the chromatographic profiles are in Figure 1BC and Suppl. Mat.

Gallic acid (**1**) was not present in the jabuticaba peel and appeared in large amounts after acid hydrolysis. Digalloylhexose (**2**) presented a similar MS pattern as compound **4** before hydrolysis (Table 1) with a parent ion at *m/z* 483 and fragment ions at *m/z* 331, 313 and 169. Its resistance to acid hydrolysis points to the presence of C-glycosidic linkages. The dehydrated form of gallic acid *C*-hexoside (**3**) was identified with a parent ion at *m/z* 313 and a fragment at *m/z* 169 for gallic acid. A parent ion at *m/z* 181 and fragments at *m/z* 137 and 109 as for the standard allowed the identification of dihydroxyphenylpropionic acid (**4**).

Newly formed compounds **14** and **15** were tentatively assigned as valoneic acid dilactone and sanguisorbic acid dilactone, respectively. Sanguisorbic acid dilactone presented a parent ion at *m/z* 469 and fragments at *m/z* 425, 301 and 299 as observed from sanguisorbic acid dilactone obtained from hydrolysis of strawberry (Mattila and Kumpulainen, 2002). Additionally, valoneic acid dilactone eluted earlier than sanguisorbic acid dilactone and presented fragments at *m/z* 425, 407 and 301 as in pomegranate (Garcia-Villalba et al., 2015). Contents in valoneic acid dilactone were 3 to 4-fold higher than contents in sanguisorbic acid dilactone in both DJP and the DJP-US extract.

No gallagic acid dilactone was found to form after 24 h of hydrolysis in contrast to pomegranate peel (García-Villalba et al., 2015). Compounds **7**, **11**, **15**, **33**, **38** and **52** (Table 1) were without ambiguity assessed as HHDP-tergalloylhexoses rather than gallagylgalloylhexoses and amounted to 0.55 mg/g of DJP after conventional extraction and 1.03 mg/g after ultrasound

extraction. Therefore, hexose acylated with the gallagyl group as in pedunculagin III, punicalagin and punicalin remains typical of pomegranate ellagitannins (García-Villalba et al., 2015). Similarly, **51** and **57** should be HHDP-galloyltergalloylhexoses while **53** and **56** ditergalloylhexoses. Additionally, various *C*-hexosides of valoneic/sanguisorbic acid dilactone or tergallic acid formed in tiny amounts and could not be quantified in this work (**7**, **9**, **11**, **12** and **13**) (Table 2). Castalagin and vescalagin are expected to release tergalloyl-*C*-glucose after acid hydrolysis while alnusiin will give valoneic acid dilactone.

Ellagic acid (**16**) was the most intense peak from pellet washing. Four HHDP-ellagic acid derivatives were identified (**5**, **6**, **8**, **10**) with parent ions at *m/z* 783 and fragmentation indicating the loss of HHDP/ellagic acid ([M-302-H]$^-$ at *m/z* 481 and fragment at *m/z* 301). One of the substituent must be ellagic acid rather than HHDP as these compounds absorb between 365 and 375 nm. They could be *C*-hexosides rather than *O*-hexosides as they are resistant to acid hydrolysis and are likely arising from a rearrangement of the five di-HHDP hexosides detected at different retention times in peel (Table 1).

Most abundant hydrolysis compounds are in decreasing order: gallic acid *C*-hexoside (**3**), ellagic acid (**16**), gallic acid (**1**) and valoneic acid dilactone (**14**). Gallic acid amounted to 11.4 mg/g in DJP and 6.3 mg/g after ultrasound extraction. The content in ellagic acid increased upon hydrolysis from 1.1 to 16.4 mg/g for DJP and from 1.1 to 10.9 mg/g after ultrasound treatment. These values agree well with that found by Alezandro, Dube et al. (2013) after acid hydrolysis of DJP (22.5 mg/g DJP). Largely lower contents in gallic acid (0.4 and 1.5 mg/g DJP, respectively) and ellagic acid (0.3 and 2.8 mg/g DJP, respectively) were found by Quatrin et al. (2019) and Inada et al. (2015) after polyphenol extraction and subsequent alkaline and acid hydrolyses of the residue supporting the degradation of the oxidizable trihydroxyphenyl moiety in basic conditions.

Overall, hydrolytic products of ellagitannins amounted to 70.3 mg/g DJP (no extraction) and 42.4 mg/g DJP after ultrasound extraction. This difference was likely due to incomplete extraction by EtOH:water (1:1) of phenolic compounds which are rather hydrophobic or bound to cell wall

18

polysaccharides and proteins. These amounts are markedly higher than those obtained by summing individual compounds from UPLC analysis (10.3 and 6.0 mg/g DJP after ultrasound and solvent extractions, respectively, and subtraction of anthocyanins and flavonols in Table 2). Acid hydrolysis, which relies on the titration of two standards ellagic acid and gallic acid, appears by far more accurate than UPLC in the absence of individual standards. Subsequent washing of the pellet with MeOH/DMSO provided one third of the hydrolysis products. It is worth noting that hydrophobic molecules such as ellagic acid and valoneic acid dilactone were mainly recovered using this additional step whereas sanguisorbic acid dilactone was only soluble in this solvent system.

3.3 Inhibition of lipid oxidation by the DJP-US extract and cyanidin-3-*O*-glucoside in *in vitro* gastrointestinal digestion

The lipid oxidation initiated by metmyoglobin (MbFe^{III}) of a 10% oil-in-water emulsion stabilized by egg yolk phospholipids was used to simulate the digestion of a Western type diet rich in ω-6 polyunsaturated lipids (Gobert et al., 2014). Initial gastric digestion is characterized by a fast rise in pH after meal intake. Then pH almost linearly decays returning to a basal pH of 2 after gastric emptying. Although static modeling cannot reproduce pH kinetics, two one hour-periods were sequentially run in this work, one at pH 5 and the other at pH 3. Conjugated dienes (CD), consisting mainly of the lipid-derived hydroperoxides formed in the propagation step of the lipid oxidation process, were followed as primary markers. Secondary marker 4-hydroxy-2-nonenal (4-HNE) was selected as a specific end-product of the oxidation of ω-6 lipids.

3.3.1 Lipid oxidation in the absence of antioxidant

In the control experiment, CD and 4-HNE accumulated in a similar linear pattern yielding 28 μmoles of CD/g of lipids and 86 nmoles of 4-HNE/g of lipids after 2 hours of gastric digestion (Fig. 2AB). The low 4-HNE/CD ratio of 3 to 1000 observed at this stage can be explained by the

465 formation of various other secondary oxidation products such as short-chain aldehydes, epoxides

466 and alcohols as well as by the high reactivity of 4-HNE. Electrophilic 4-HNE reacts rapidly with

467 nucleophilic cysteine, histidine and lysine residues in proteins as already evidenced in pig gastric

468 digesta (Delosiere et al., 2016). Increase of pH at 6.5 and addition of bile and pancreatin induced an

469 apparent drop in lipid oxidizability in the early intestinal phase. A CD faster degradation or an

470 incomplete extraction of lipids from the mixed micelles by the 2-propanol/hexane system could

471 explain this apparent CD loss. As to 4-HNE, it disappeared almost totally. Then, CD and 4-HNE

472 exhibited different patterns in the intestinal step. CD kept accumulating reaching 40 µmoles/g lipids

473 at the end of the intestinal step. In contrast to the concomitant formation of 4-HNE and CD in the

474 gastric phase, free 4-HNE only weakly accumulated reaching 7.5 µmoles per g lipids after 240 min.

475 Additional proteins and enzymes from bile and pancreatin may have reacted with continuously

476 formed 4-HNE.

477

478 *3.3.2 Lipid oxidation in the presence of the DJP-US extract and cyanidin-3-O-glucoside*

479 The DJP-US extract and C3G were evaluated as inhibitors of lipid oxidation at similar anthocyanin

480 concentrations although anthocyanins in the ultrasonic extract were constituted by 89% of C3G and

481 11% of D3G. Five-fold higher levels in anthocyanins were brought through US-5 and C3G-5

482 compared to US-1 and C3G-1.

483 In the gastric step, the addition of C3G slowed down CD accumulation in a concentration-

484 dependent manner with a significant effect ($p = 0.05$) for both levels between 90 and 120 min. After

485 2 h of gastric digestion, CD inhibition was of 52% and 65% for C3G-1 and C3G-5, respectively.

486 Interestingly, US-1 and US-5 extracts afforded a largely higher protection with inhibition rates of

487 87% and 100%, respectively. This difference was also outlined for the accumulation of 4-HNE. As

488 a matter of fact, C3G-1 and C3G-5 significantly inhibited 4-HNE formation between 90 and 120

489 min while being significantly less antioxidant than the two concentrations used for the DJP-US

490 extract. Inhibition rates were 28% and 55% for C3G-1 and C3G-5 while 91% and 97% for US-1

491   and US-5. With pure C3G, 30 and 60 min-long lag phases were evidenced and found consistent

492   with remaining C3G during these periods (Fig. 3).

493   After 30 min of intestinal digestion, the DJP-US extracts appeared unexpectedly unable to inhibit

494   the accumulation of CD with apparent rates almost faster than for control. In contrast, the less

495   antioxidant C3G-1 and C3G-5 kept their inhibitory action throughout the intestinal phase. This

496   unexpected increase in CD with the DJP-US extracts may be ascribed to the extraction by the 2-

497   propanol/hexane mixture of amino acids or small peptides released through proteolysis of the

498   jabuticaba peel extract and absorbing at 234 nm. This apparent loss of activity has also been

499   observed for apple puree and extract (unpublished data). Epicatechin used for comparison strongly

500   inhibited CD accumulation as evidenced here with C3G. Primary lipid oxidation products should be

501   assessed with a different method because of the possible interferences at 234 nm from complex

502   plant products.

503   As observed earlier for control, no clear accumulation of 4-HNE occurred in the intestinal step in

504   agreement with the likely fast reaction of this marker with digestive proteins at a higher pH.

505

506   **3.4   Bioaccessibility of anthocyanins**

507   Only anthocyanins could be recovered during the digestion of phospholipid-stabilized emulsions

508   under oxidative stress. Other phenolic compounds from the DJP-US extracts were present at too

509   low levels to be quantified.

510   In the gastric step, pure C3G disappeared very fast from the aqueous phase since only 14% were

511   recovered for the highest concentration at 30 min and 0% for the lowest concentration. By contrast,

512   C3G from US-1 and US-5 was largely present at the end of the gastric step with recovery rates of

513   21% and 72%. Less abundant D3G could only be recovered from US-5 at a rate of 22%. This lower

514   recovery is mainly due to the higher oxidizability of the 1,2,3-trihydroxyphenyl moiety of

515   delphinidin when compared to that of the 1,2-dihydroxyphenyl nucleus of cyanidin. Similarly,

516 Quatrin et al. (2020) showed a higher recovery of C3G (85%) than D3G (71%) at the end of the

517 gastric step for a jabuticaba peel powder.

518 The 5 min-long transition from the gastric to the intestinal phase led to a complete disappearance of

519 C3G from US-1 and D3G from US-5. C3G from US-5 dropped to 26% during this short period

520 before totally disappearing. As sample acidification was conducted before anthocyanin

521 quantification, the decays observed suggest a degradation of the flavylium nucleus as a result of

522 both antioxidant action and unfavorable near neutral conditions.

523

524 **4. Discussion**

525 **Lipid oxidation and inhibition in gastrointestinal digestion**

526 Chemical reactions and physicochemical interactions occurring between bolus constituents

527 should be unraveled to shed some light on the bioavailability of plant secondary metabolites and

528 their health benefit directly in the gastrointestinal tract. Digestion modeling allows to take into

529 account both human food and physiological conditions of digestion. An average Western adult daily

530 consumes 100 to 150 g of triglycerides and 2 to 10 g of phospholipids. After gastric antral

531 contractions, dietary lipids are recovered in the emulsion form with most of the lipid droplets in the

532 1-50 µm diameter range (Lorrain, Dangles, Genot, & Dufour, 2010). A 12.5% oil-in water emulsion

533 stabilized by egg yolk PL and characterized by a single mode at 14.8 ± 0.3 µm and a D(3,2) at 1.09

534 ± 0.18 µm was thus prepared as food model. While simulated fluids, enzymes (1000 U pepsin/mL,

535 100 U trypsin/mL) and bile levels were as proposed by Minekus et al. (2014), the gastric pH was

536 more physiologically simulated with a pH jump from 5 to 3 after one hour.

537 The heme iron form of red meat, metmyoglobin, was added at a 30 µM level in the gastric

538 step simulating the consumption of 85 g of beef steak (chyme volume of 1 L). Metmyoglobin-

539 initiated oxidation of polyunsaturated fatty acid led to the formation of lipid-derived conjugated

540 dienes and 4-HNE as primary and end markers, respectively (Fig. 2AB). The change in pH from 5

541 to 3 appeared to increase both rates of accumulation. As a matter of fact, the proteolysis of

22

metmyoglobin by pepsin has been evidenced at pH 5 although this process is faster at lower pHs (Bolea et al., 2019). The resulting micro-metmyoglobin can accelerate lipid oxidation likely due to a facilitated access for lipids to the iron center. Then, pH lowering leads to the formation of an unfolded form of metmyoglobin which appeared to be stable during at least 30 min at pH 3. The release of hematin from proteolyzed unfolded metmyoglobin at pH 3, although suggested by some authors, is still unclear by now. Whatever the heme iron form, lipid oxidation proceeded at both gastric pHs suggesting that this deleterious process is susceptible to degrade essential ω-6 lipids *in vivo*.

Thus, it is critical to identify protective food that, when co-ingested, could limit lipid oxidation in the GIT and the onset of cardiovascular diseases in a longer term. In this work, the effect of a jabuticaba peel rich in anthocyanins and hydrolyzable tannins was compared to that of a pure anthocyanin, C3G. At identical anthocyanin contents, the DJP-US extracts more extensively inhibited the accumulation of CD and 4-HNE than C3G-1 and C3G-5. This difference was particularly significant at 90 and 120 min of gastric digestion for 4-HNE ($p < 0.05$) and at 60, 90 and 120 min for CD (Fig. 2AB). C3G-1 and C3G-5 were found to inhibit the accumulation of the primary marker CD in a concentration-dependent manner while totally inhibiting that of 4-HNE during lag phases that correlate with the presence of C3G in the digesta. After the disappearance of C3G, 4-HNE formed at rates that are lower than observed for control suggesting an additional antioxidant effect of the degradation products of C3G. In the pH range of 2 to 4 or in oxidative conditions at pH 7, cyanidin glycosides were reported to be degraded into protocatechuic acid, phloroglucinaldehyde and 3,5,7-trihydroxycoumarin among others (Dangles & Fenger, 2018). Protocatechuic acid, which is also a metabolite from quercetin oxidation, could contribute to the antioxidant capacity of C3G as previously demonstrated for quercetin (Lorrain et al., 2010).

The almost total inhibition of lipid oxidation in the presence of US-5 is consistent with the high rate of remaining anthocyanins, found to be 72% for C3G and 22% for D3G, after the gastric step (Fig. 3). The potent capacity of the DJP-US extract can also be attributed to the additional presence of

hydrolyzable tannins and flavonols which constitute 84% and 0.5% of the phenolic pool of the jabuticaba peel extract (evaluation after acid hydrolysis). All of these compounds display the typical 1,2-dihydroxy- and 1,2,3-trihydroxyphenyl moieties that are critical to the reducing capacity of phenolic compounds.

In the intestinal phase at pH 6.5, the formation of lipid-derived conjugated dienes was demonstrated for the first time suggesting that the heme iron form maintains its prooxidant activity towards triacylglycerols and their lipolytic products. Those are mainly monoacylglycerols and free fatty acids solubilized in mixed micelles with biliary salts. Although this work did not allow to evidence the accumulation of 4-HNE because of its rapid scavenging by peptides and proteins, primary lipid oxidation products are known to be unstable in intestinal conditions. Indeed, the *in vitro* digestion of a thermodegraded sunflower oil generated hexanal and nonanal as the major alkenals while 2-heptenal and 2-octenal were recovered in higher rates than 4-HNE (Goicoechea et al., 2008). Moreover, Kanazawa & Ashida (1998) identified uncleaved epoxyketones, 9-oxononanoic acid and hexanal in the intestinal lumen of rats fed with linoleyl hydroperoxides. 4-HNE is absorbable and can be recovered under various metabolized forms (Keller, Baradat, Jouanin, Debrauwer, & Gueraud, 2015). By covalently reacting with the ApoB protein of LDL, 4-HNE is involved in the formation of atherogenic oxLDL particles. Furthermore, 4-HNE appears to play a role in the development of colonic preneoplastic lesions (Bastide et al., 2017).

Bioaccessibility and reactivity of anthocyanins and hydrolyzable tannins

Diet-induced oxidative stress led to the fast disappearance of C3G during gastric digestion. Anthocyanins can play an antioxidant role in metmyoglobin-initiated lipid oxidation by reducing the ferrylmyoglobin initiating species rather than the propagating peroxyl radicals (Goupy, Bautista-Ortin, Fulcrand, & Dangles, 2009). Interestingly, hydrolyzable tannins, which are present in a 5-fold excess compared to anthocyanins in the DJP-US extract, had the ability to slow down their degradation. Hydrolyzable tannins were constituted for half by HHDP-galloylhexose **2**, ellagic acid

24

42, HHDP-digalloylhexoses **29** and **37**, tetragalloylhexose **46**, pentagalloylhexose **50**, HHDP-tergalloylhexose **38**, and di-HHDP-hexoses **10** and **17**, in decreasing order. This composition agrees well with results from Plaza et al. (2016) and Quatrin et al. (2019). The possible interaction of these high-molecular weight compounds with the iron-oxo center of ferrylmyoglobin is suggested by the superior antioxidant activity of the extracts. Furthermore, ellagitannins and gallotannins are prone to degradation in *in vitro* gastrointestinal digestion, yielding mainly gallic acid and ellagic acid for a jabuticaba peel powder (Quatrin et al., 2020). Their stability was mostly affected by intestinal conditions which also led to the total disappearance of anthocyanins while only lightly affecting flavonols. A matrix effect should also be taken into consideration when investigating extracts and peel powders (Quatrin et al., 2020; Peixoto et al., 2016). Binding to cell wall polysaccharides and proteins is expected to slow polyphenol diffusion out of the matrix increasing thus their life time.

Conclusion

Jabuticaba peel hydroalcoholic extracts exhibit high potency in limiting the formation of deleterious lipid hydroperoxides and aldehydes arising from diet-induced oxidation of essential ω-6 lipids in the gastrointestinal tract. This inhibitory capacity can be ascribed to high levels in antioxidant anthocyanins (1% DM) and hydrolyzable tannins (7% DM), thus pointing to promising future uses for jabuticaba extracts as food ingredient or colorant.

Conflicts of interest

There are no conflicts of interest to declare.

25

622

623

References

Albuquerque, B. R., Pereira, C., Calhelha, R. C., José Alves, M., Abreu, R. M. V., Barros, L., Oliveira, M. B. P. P., & Ferreira, I. C. F. R. (2020). Jabuticaba residues (Myrciaria jaboticaba (Vell.) Berg) are rich sources of valuable compounds with bioactive properties. *Food Chemistry, 309*, 125735.

Alezandro, M. R., Dube, P., Desjardins, Y., Lajolo, F. M., & Genovese, M. I. (2013). Comparative study of chemical and phenolic compositions of two species of jaboticaba: Myrciaria jaboticaba (Vell.) Berg and Myrciaria cauliflora (Mart.) O. Berg. *Food Research International, 54*(1), 468-477.

Alezandro, M. R., Granato, D., & Genovese, M. I. (2013). Jaboticaba (Myrciaria jaboticaba (Vell.) Berg), a Brazilian grape-like fruit, improves plasma lipid profile in streptozotocin-mediated oxidative stress in diabetic rats. *Food Research International, 54*(1), 650-659.

Baldin, J. C., Michelin, E. C., Polizer, Y. J., Rodrigues, I., de Godoy, S. H. S., Fregonesi, R. P., Pires, M. A., Carvalho, L. T., Fávaro-Trindade, C. S., de Lima, C. G., Fernandes, A. M., & Trindade, M. A. (2016). Microencapsulated jabuticaba (Myrciaria cauliflora) extract added to fresh sausage as natural dye with antioxidant and antimicrobial activity. *Meat Science, 118*, 15-21.

Bastide, N. M., Naud, N., Nassy, G., Vendeuvre, J. L., Tache, S., Gueraud, F., Hobbs, D. A., Kuhnle, G. G., Corpet, D. E., & Pierre, F. H. F. (2017). Red wine and pomegranate extracts suppress cured meat promotion of colonic mucin-depleted foci in carcinogen-induced rats. *Nutrition and Cancer, 69*(2), 289-298.

Bolea, G., Ginies, C., Vallier, M. J., & Dufour, C. (2019). Lipid protection by polyphenol-rich apple matrices is modulated by pH and pepsin in in vitro gastric digestion. *Food & Function, 10*(7), 3942-3954.

Bolea, G., Philouze, C., Dubois, M., Risdon, S., Humberclaude, A., Ginies, C., Charles, A. L., Geny, B., Reboul, C., Arnaud, C., Dufour, C., & Meyer, G. (2021). Digestive n-6 lipid oxidation, a key trigger of vascular dysfunction and atherosclerosis in the Western diet: protective effects of apple polyphenols. *Molecular Nutrition & Food Research, accepted, 10.1002/mnfr.202000487*.

Calani, L., Beghe, D., Mena, P., Del Rio, D., Bruni, R., Fabbri, A., Dall'Asta, C., & Galaverna, G. (2013). Ultra-HPLC MSn (poly)phenolic profiling and chemometric analysis of juices from ancient Punica granatum L. cultivars: a nontargeted approach. *Journal of Agricultural and Food Chemistry, 61*(23), 5600-5609.

Dangles, O., & Fenger, J. A. (2018). The chemical reactivity of anthocyanins and its consequences in food science and nutrition. *Molecules, 23*(8).

de Ferrars, R. M., Czank, C., Zhang, Q., Botting, N. P., Kroon, P. A., Cassidy, A., & Kay, C. D. (2014). The pharmacokinetics of anthocyanins and their metabolites in humans. *British Journal of Pharmacology, 171*(13), 3268-3282.

Delosiere, M., Sante-Lhoutellier, V., Chantelauze, C., Durand, D., Thomas, A., Joly, C., Pujos-Guillot, E., Remond, D., Comte, B., Gladine, C., Guy, A., Durand, T., Laurentie, M., & Dufour, C. (2016). Quantification of 4-hydroxy-2-nonenal-protein adducts in the in vivo gastric digesta of mini-pigs using a GC-MS/MS method with accuracy profile validation. *Food & Function, 7*(8), 3497-3504.

Fairlie-Jones, L., Davison, K., Fromentin, E., & Hill, A. M. (2017). The effect of anthocyanin-rich foods or extracts on vascular function in adults: a systematic review and meta-analysis of randomised controlled trials. *Nutrients, 9*(8), 908.

Fischer, U. A., Carle, R., & Kammerer, D. R. (2011). Identification and quantification of phenolic compounds from pomegranate (Punica granatum L.) peel, mesocarp, aril and differently produced juices by HPLC-DAD-ESI/MSn. *Food Chemistry, 127*(2), 807-821.

667 Fracassetti, D., Costa, C., Moulay, L., & Tomas-Barberan, F. A. (2013). Ellagic acid derivatives, ellagitannins,
668   proanthocyanidins and other phenolics, vitamin C and antioxidant capacity of two powder products
669   from camu-camu fruit (Myrciaria dubia). *Food Chemistry, 139*(1-4), 578-588.
670 Garcia-Conesa, M. T., Chambers, K., Combet, E., Pinto, P., Garcia-Aloy, M., Andres-Lacueva, C., de Pascual-
671   Teresa, S., Mena, P., Ristic, A. K., Hollands, W. J., Kroon, P. A., Rodriguez-Mateos, A., Istas, G.,
672   Kontogiorgis, C. A., Rai, D. K., Gibney, E. R., Morand, C., Espin, J. C., & Gonzalez-Sarrias, A. (2018).
673   Meta-analysis of the effects of foods and derived products containing ellagitannins and
674   anthocyanins on cardiometabolic biomarkers: analysis of factors influencing variability of the
675   individual responses. *International Journal of Molecular Sciences, 19*(3).
676 Garcia-Villalba, R., Espin, J. C., Aaby, K., Alasalvar, C., Heinonen, M., Jacobs, G., Voorspoels, S., Koivumaki,
677   T., Kroon, P. A., Pelvan, E., Saha, S., & Tomas-Barberan, F. A. (2015). Validated method for the
678   characterization and quantification of extractable and nonextractable ellagitannins after acid
679   hydrolysis in pomegranate fruits, juices, and extracts. *Journal of Agricultural and Food Chemistry,*
680   *63*(29), 6555-6566.
681 Gobert, M., Remond, D., Loonis, M., Buffiere, C., Sante-Lhoutellier, V., & Dufour, C. (2014). Fruits,
682   vegetables and their polyphenols protect dietary lipids from oxidation during gastric digestion.
683   *Food & Function, 5*, 2166-2174.
684 Goicoechea, E., Van Twillert, K., Duits, M., Brandon, E., Kootstra, P. R., Blokland, M. H., & Guillen, M. D.
685   (2008). Use of an in vitro digestion model to study the bioaccessibility of 4-hydroxy-2-nonenal and
686   related aldehydes present in oxidized oils rich in omega-6 acyl groups. *Journal of Agricultural and*
687   *Food Chemistry, 56*(18), 8475-8483.
688 Goupy, P., Bautista-Ortin, A. B., Fulcrand, H., & Dangles, O. (2009). Antioxidant activity of wine pigments
689   derived from anthocyanins: hydrogen transfer reactions to the DPPH radical and inhibition of the
690   heme-induced peroxidation of linoleic acid. *Journal of Agricultural and Food Chemistry, 57*(13),
691   5762-5770.
692 Inada, K. O. P., Oliveira, A. A., Revoredo, T. B., Martins, A. B. N., Lacerda, E. C. Q., Freire, A. S., Braz, B. F.,
693   Santelli, R. E., Torres, A. G., Perrone, D., & Monteiro, M. C. (2015). Screening of the chemical
694   composition and occurring antioxidants in jabuticaba (Myrciaria jaboticaba) and jussara (Euterpe
695   edulis) fruits and their fractions. *Journal of Functional Foods, 17*, 422-433.
696 Kanazawa, K., & Ashida, H. (1998). Dietary hydroperoxides of linoleic acid decompose to aldehydes in
697   stomach before being absorbed into the body. *Biochimica Et Biophysica Acta-Lipids and Lipid*
698   *Metabolism, 1393*(2-3), 349-361.
699 Keller, J., Baradat, M., Jouanin, I., Debrauwer, L., & Gueraud, F. (2015). "Twin peaks": Searching for 4-
700   hydroxynonenal urinary metabolites after oral administration in rats. *Redox Biology, 4*, 136-148.
701 Leite-Legatti, A. V., Batista, A. G., Dragano, N. R. V., Marques, A. C., Malta, L. G., Riccio, M. F., Eberlin, M. N.,
702   Machado, A. R. T., de Carvalho-Silva, L. B., Ruiz, A., de Carvalho, J. E., Pastore, G. M., & Marostica,
703   M. R. (2012). Jaboticaba peel: Antioxidant compounds, antiproliferative and antimutagenic
704   activities. *Food Research International, 49*(1), 596-603.
705 Lenquiste, S. A., Lamas, C. D., Marineli, R. D., Moraes, E. A., Borck, P. C., Camargo, R. L., Quitete, V.,
706   Carneiro, E. M., & Marostica, M. R. (2019). Jaboticaba peel powder and jaboticaba peel aqueous
707   extract reduces obesity, insulin resistance and hepatic fat accumulation in rats. *Food Research*
708   *International, 120*, 880-887.
709 Lorrain, B., Dangles, O., Genot, C., & Dufour, C. (2010). Chemical modeling of heme-induced lipid oxidation
710   in gastric conditions and inhibition by dietary polyphenols. *Journal of Agricultural and Food*
711   *Chemistry, 58*(1), 676-683.
712 Marques Peixoto, F., Fernandes, I., Gouvêa, A. C. M. S., Santiago, M. C. P. A., Galhardo Borguini, R., Mateus,
713   N., Freitas, V., Godoy, R. L. O., & Ferreira, I. M. P. L. V. O. (2016). Simulation of in vitro digestion
714   coupled to gastric and intestinal transport models to estimate absorption of anthocyanins from
715   peel powder of jabuticaba, jamelão and jambo fruits. *Journal of Functional Foods, 24*, 373-381.
716 Mattila, P., & Kumpulainen, J. (2002). Determination of free and total phenolic acids in plant-derived foods
717   by HPLC with diode-array detection. *Journal of Agricultural and Food Chemistry, 50*(13), 3660-3667.
718

Mena, P., Calani, L., Dall'Asta, C., Galaverna, G., Garcia-Viguera, C., Bruni, R., Crozier, A., & Del Rio, D. (2012). Rapid and Comprehensive Evaluation of (Poly)phenolic Compounds in Pomegranate (Punica granatum L.) Juice by UHPLC-MSn. *Molecules*, *17*(12), 14821-14840.

Minekus, M., Alminger, M., Alvito, P., Ballance, S., Bohn, T., Bourlieu, C., Carriere, F., Boutrou, R., Corredig, M., Dupont, D., Dufour, C., Egger, L., Golding, M., Karakaya, S., Kirkhus, B., Le Feunteun, S., Lesmes, U., Macierzanka, A., Mackie, A., Marze, S., McClements, D. J., Menard, O., Recio, I., Santos, C. N., Singh, R. P., Vegarud, G. E., Wickham, M. S. J., Weitschies, W., & Brodkorb, A. (2014). A standardised static in vitro digestion method suitable for food - an international consensus. *Food & Function, 5*, 1113-1124.

Morales, P., Barros, L., Dias, M. I., Santos-Buelga, C., Ferreira, I., Asquieri, E. R., & Berrios, J. D. (2016). Non-fermented and fermented jabuticaba (Myrciaria cauliflora Mart.) pomaces as valuable sources of functional ingredients. *Food Chemistry, 208*, 220-227.

Neves, N. d. A., Stringheta, P. C., Gómez-Alonso, S., & Hermosín-Gutiérrez, I. (2018). Flavonols and ellagic acid derivatives in peels of different species of jabuticaba (Plinia spp.) identified by HPLC-DAD-ESI/MSn. *Food Chemistry, 252*, 61-71.

Pereira, L. D., Barbosa, J. M. C., da Silva, A. J. R., Ferri, P. H., & Santos, S. C. (2017). Polyphenol and Ellagitannin Constituents of Jabuticaba (Myrciaria cauliflora) and Chemical Variability at Different Stages of Fruit Development. *Journal of Agricultural and Food Chemistry, 65*(6), 1209-1219.

Plaza, M., Batista, A. G., Cazarin, C. B. B., Sandahl, M., Turner, C., Ostman, E., & Marostica, M. R. (2016). Characterization of antioxidant polyphenols from Myrciaria jaboticaba peel and their effects on glucose metabolism and antioxidant status: A pilot clinical study. *Food Chemistry, 211*, 185-197.

Quatrin, A., Pauletto, R., Maurer, L. H., Minuzzi, N., Nichelle, S. M., Carvalho, J. F. C., Marostica, M. R., Rodrigues, E., Bochi, V. C., & Emanuelli, T. (2019). Characterization and quantification of tannins, flavonols, anthocyanins and matrix-bound polyphenols from jaboticaba fruit peel: A comparison between Myrciaria trunciflora and M. jaboticaba. *Journal of Food Composition and Analysis, 78*, 59-74.

Quatrin, A., Rampelotto, C., Pauletto, R., Maurer, L. H., Nichelle, S. M., Klein, B., Rodrigues, R. F., Marostica, M. R., Fonseca, B. D., de Menezes, C. R., Mello, R. D., Rodrigues, E., Bochi, V. C., & Emanuelli, T. (2020). Bioaccessibility and catabolism of phenolic compounds from jaboticaba (Myrciaria trunciflora) fruit peel during in vitro gastrointestinal digestion and colonic fermentation. *Journal of Functional Foods, 65*.

Silva, R. M., Pereira, L. D., Veras, J. H., do Vale, C. R., Chen-Chen, L., & Santos, S. D. (2016). Protective effect and induction of DNA repair by Myrciaria cauliflora seed extract and pedunculagin on cyclophosphamide-induced genotoxicity. *Mutation Research-Genetic Toxicology and Environmental Mutagenesis, 810*, 40-47.

Tanaka, T., Tong, H. H., Xu, Y. M., Ishimaru, K., Nonaka, G., & Nishioka, I. (1992). Tannins and related-compounds.117. Isolation and characterization of 3 new ellagitannins, lagerstannins A, B and C, having a gluconic acid core, from Lagerstroemia-speciosa (L) pers. *Chemical & Pharmaceutical Bulletin, 40*(11), 2975-2980.

Tarone, A. G., Silva, E. K., Barros, H., Cazarin, C. B. B., & Marostica, M. R. (2021). High-intensity ultrasound-assisted recovery of anthocyanins from jabuticaba by-products using green solvents: Effects of ultrasound intensity and solvent composition on the extraction of phenolic compounds. F*ood Research International, 140*, 110048.

Tarone, A. G., Silva, E. K., Cazarin, C. B. B., & Marostica, M. R. (2021). Inulin/fructooligosaccharides/pectin-based structured systems: Promising encapsulating matrices of polyphenols recovered from jabuticaba peel. *Food Hydrocolloids, 111*, 106387.

Tavares, I. M. d. C., Lago-Vanzela, E. S., Rebello, L. P. G., Ramos, A. M., Gómez-Alonso, S., García-Romero, E., Da-Silva, R., & Hermosín-Gutiérrez, I. (2016). Comprehensive study of the phenolic composition of the edible parts of jambolan fruit (Syzygium cumini (L.) Skeels). *Food Research International, 82*, 1-13.

769   Wang, P., Cheng, C., Ma, Y., & Jia, M. (2020). Degradation behavior of polyphenols in model aqueous

770   extraction system based on mechanical and sonochemical effects induced by ultrasound.

771   *Separation and Purification Technology, 247*, 116967.

772   Wu, S. B. A., Dastmalchi, K., Long, C. L., & Kennelly, E. J. (2012). Metabolite profiling of jaboticaba (Myrciaria

773   cauliflora) and other dark-colored fruit juices. *Journal of Agricultural and Food Chemistry, 60*(30),

774   7513-7525.

775
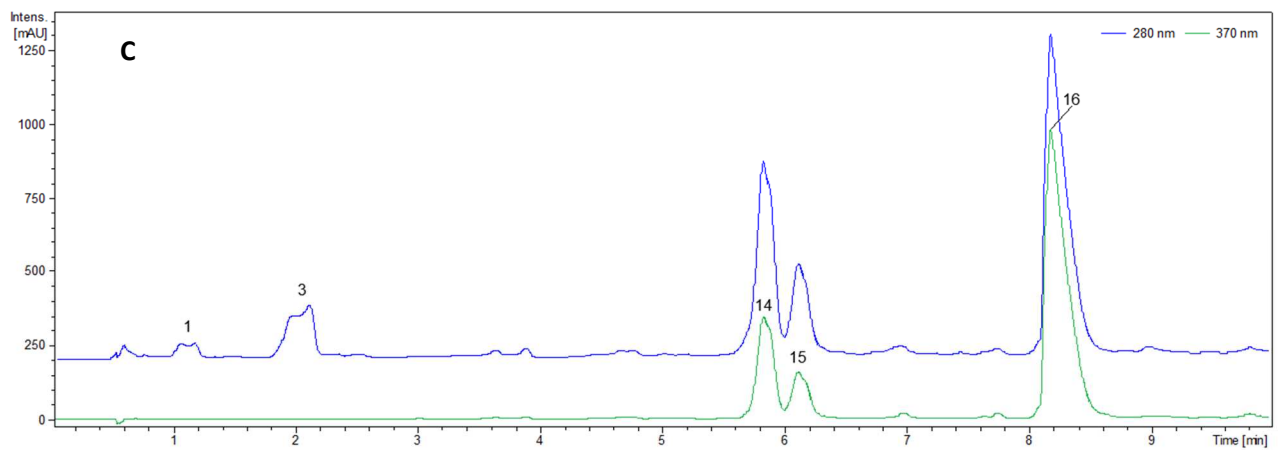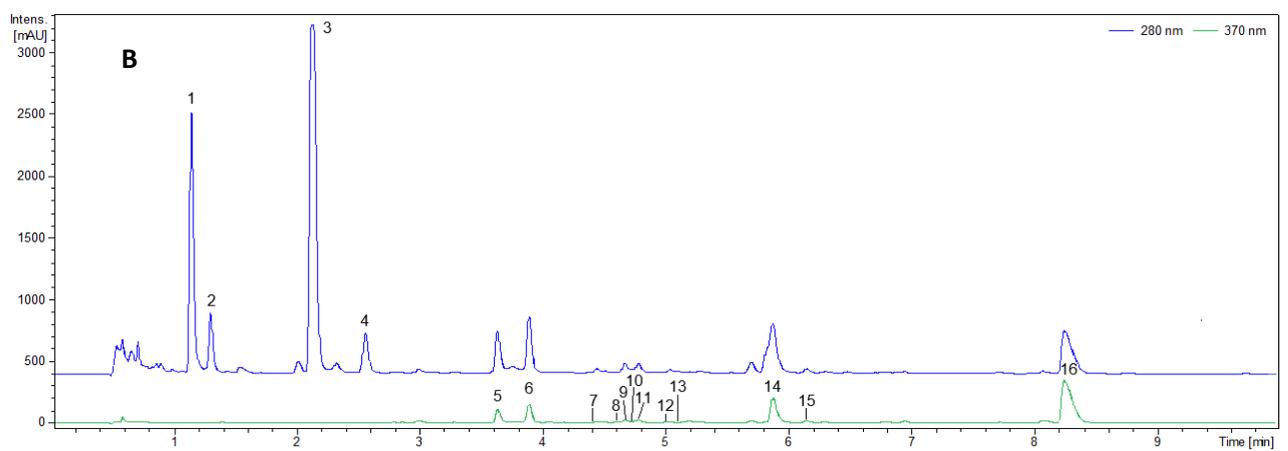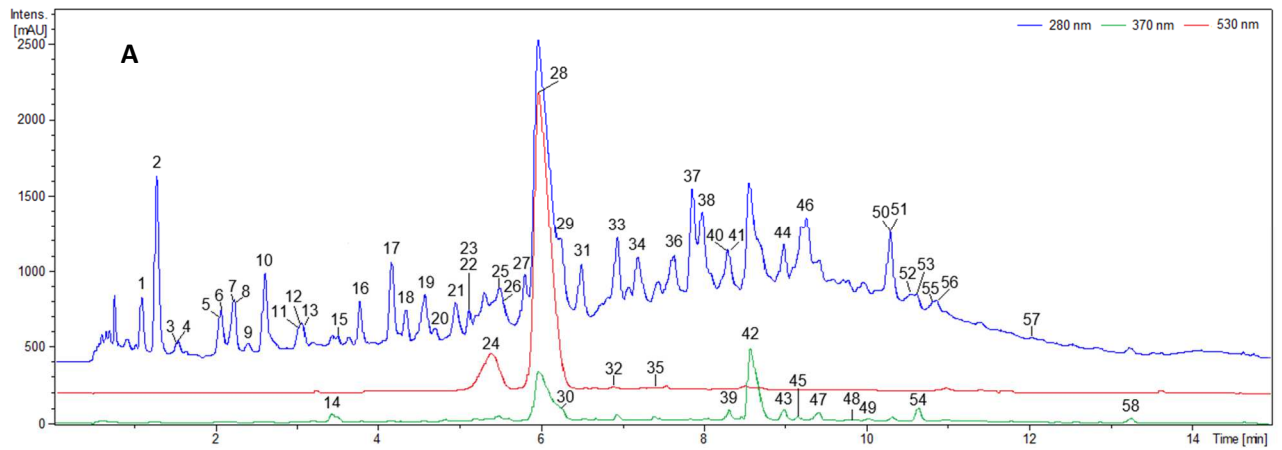
Figure 1. Chromatographic profile of the phenolic compounds for the DJP-US extract before hydrolysis at 280 nm, 370 nm and 530 nm (A) and after hydrolysis at 280 nm and 370 nm (B – Supernatant and C – Pellet washing).
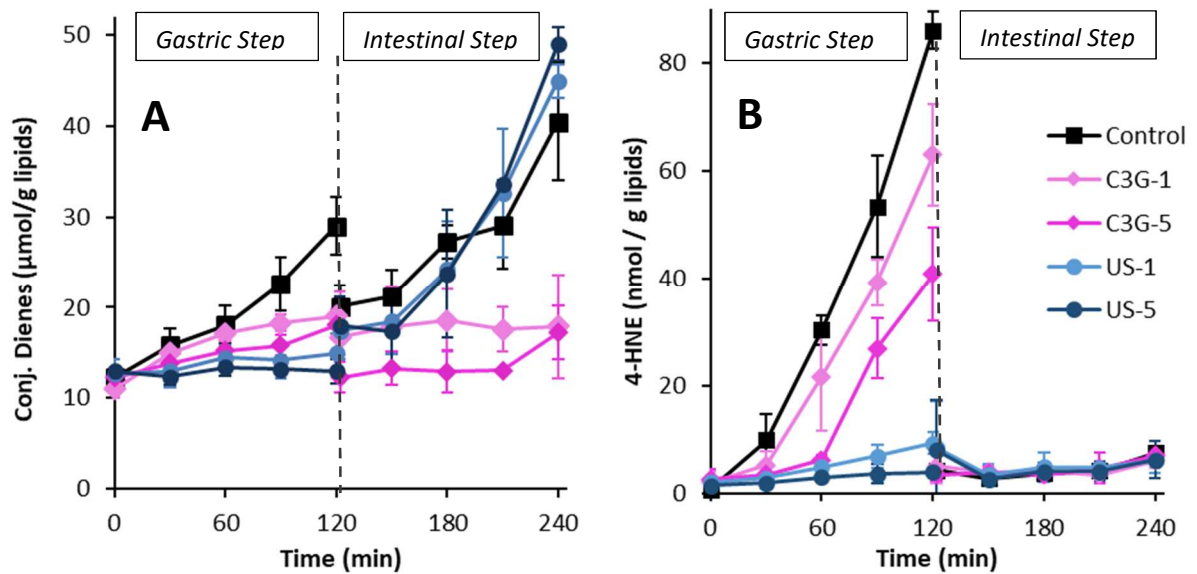
Figure 2: Inhibition by the DJP-US extract and pure C3G of the accumulation of (A) lipid-derived conjugated dienes (CD) and (B) 4-HNE during the *in vitro* simulated digestion of phospholipid-stabilized emulsions. US-1 and C3G-1 bring 14.9 µg total anthocyanins while US-5 and C3G-5 74.4 µg. Lipid oxidation was initiated by metmyoglobin (30 µM). Values represent mean ± SD (n = 3–7).
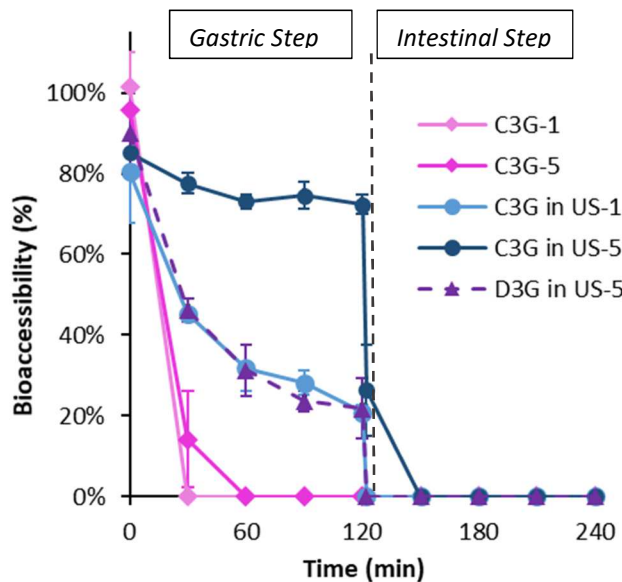
Figure 3: Bioaccessibility of C3G and D3G during the *in vitro* simulated gastrointestinal digestion of phospholipid-stabilized emulsions in the presence of metmyoglobin (30 µM) and the DJP-US extract or pure C3G. Values represent mean ± SD (n = 3).

Table 1. Phenolic compounds identified by UPLC/DAD/ESI-MS^n in dried jabuticaba peel extracts obtained by ultrasound technology and conventional solvent extraction.

| N°	RT (min)	λ_{max} (nm)	[M - H]⁻ / [M]⁺ (m/z)*	MS² fragments (m/z)	Tentative identification
1	1.1	277	331	271-**169**	Galloylhexose [a]
2	1.3	270	633	**301**-*275*-249	HHDP-galloylhexose (1) [abh]
3	1.6	266	649	**605**-481-*479*-425	HHDP-galloylgluconic acid [c]
4	1.6	266	483	**331**-313-169	Digalloylhexose (1) [ad]
5	2.1	264	633	**301**-*275-249*	HHDP-galloylhexose (2) [abh]
6	2.1	264	783	765-721-507-**481**-419-341-301-275	Di-HHDP-hexose (1) [abdhj]
7	2.2	282	933	**915**-871-613-569	HHDP-tergalloylhexose (1) [defg]
8	2.2	282	801	783-**757**-633	HHDP-digalloylgluconic acid (punigluconin) (1) [cd]
9	2.5	260	783	481-**301**-275	Di-HHDP-hexose (2) [abdhj]
10	2.7	260	783	481-**301**-275	Di-HHDP-hexose (3) [abdhj]
11	3.1	260	933	915-**631**-613-569	HHDP-tergalloylhexose (2) [adefg]
12	3.1	260	801	**757**-633	HHDP-digalloylgluconic acid (punigluconin) (2) [cd]
13	3.1	260	951	**907**-783-605-*481-405-347-301*	Di-HHDP-galloylgluconic acid (1)
14	3.5	370	469	**425**	Tergallic acid dilactone (1)
15	3.6	260	933	631-*571*-**451**-*425-301*	HHDP-tergalloylhexose (3) [adefj]
16	3.8	260	633	*615*-481-**301**-275	HHDP-galloylhexose (3) [abh]
17	4.2	260	783	481-*421*-**301**-275	Di-HHDP-hexose (4) [abdhj]
18	4.4	260	951	**907**-783-605-*481-425-361-299*	Di-HHDP-galloylgluconic acid (2)
19	4.6	260	951	**907**-783-605-*481-425-361-299*	Di-HHDP-galloylgluconic acid (3)

20	4.7	260	631	*613*-571-**451**-407-*351*	Valoneic (sanguisorbic) acid dilactone C-hexoside or Tergalloyl-O-hexose (Cauliflorin) [e] or Tergalloyl-C-hexose [a] (1)
21	5.0	270	785	633-**483**-419-*331*-301-*275*	HHDP-digalloylhexose (1) [abdfj]
22	5.1	272	483	331-**271**-169	Digalloylhexose (2) [ad]
23	5.1	272	631	613-571-**451**-407-*351*	Valoneic (sanguisorbic) acid dilactone C-hexoside or Tergalloyl-O-hexose (Cauliflorin) [e] or Tergalloyl-C-hexose [a] (2)
24	5.4	526	465*	**303***	Delphinidin-3-*O*-glucoside [abh]
25	5.6	260	633	*615-463*-**301**	HHDP-galloylhexose (4) [abhj]
26	5.7	260	935	**917**-873-855-573	Di-HHDP-galloylhexose (1) (Casuarinin/Stachyurin/Casuarictin/Potentillin) [abdefhj]
27	5.9	265	935	917-873-783-659-**633**-571-301	Di-HHDP-galloylhexose (2) (Casuarinin/Stachyurin/Casuarictin/Potentillin) [abcdefh]
28	6.2	514	449*	**287***	Cyanidin-3-*O*-glucoside (std) [abh]
29	6.3	270	785	633-**483**-*419*-301-*249*	HHDP-digalloylhexose (2) [abdfj]
30	6.3	372	469	451-**425**-407-301-*167*	Valoneic acid dilactone [cfh]
31	6.5	260	951	**907**-783-*605*	Di-HHDP-galloylgluconic acid (4)
32	6.9	516	433*	**271***	Pelargonidin-*O*-hexoside [a]
33	7.0	260	933	*763*-631-481-**451**-*425-301*	HHDP-tergalloylhexose (4) [adefj]
34	7.2	264	635	617-483-**423**-*271*	Trigalloylhexose [a]
35	7.4	524	463*	**301***	Peonidin-*O*-hexoside [a]
36	7.7	260	935	*917-765*-**633**-*615-481*-451-301	Di-HHDP-galloylhexose (3) (Casuarinin/Stachyurin/Casuarictin/potentillin) [abdf]
37	7.9	264	785	633-**483**-301	HHDP-digalloylhexose (3) [abdfj]
38	8.0	260	933	631-481-**451**-*301*	HHDP-tergalloylhexose (5) [adefj]
39	8.3	355	433	**301**-*287-273-209*	Ellagic acid pentoside [abdfh]
40	8.3	-	783	**765**-*613*-465-*451*-419-301	Di-HHDP-hexose (5) [abdh]
41	8.3	-	937	785-**767**-741-635-465-419-301-275	HHDP-trigalloylhexose [bfhj]

42	8.6	367	301	*229-185*	Ellagic acid (std) [abcdefh]
43	9.0	350	463	**317**-*237-179-151*	Myricetin deoxyhexoside [ahi]
44	9.0	264	787	635-**617**-467-447-*403*	Tetragalloylhexose (1) [ad]
45	9.2	350	463	**301**-273-*245-213-179-151*	Quercetin hexoside (1) [ai]
46	9.3	272	787	**617**-*465-449*	Tetragalloylhexose (2) [a]
47	9.4	350	463	**301**-*273-257-229-179-151*	Quercetin hexoside (2) [ai]
48	9.8	350	433	**301**-271-*257-179*	Quercetin pentoside (1) [ai]
49	10.0	350	433	**301**-*271-253-225-179-151-125*	Quercetin pentoside (2) [ai]
50	10.3	275	939	787-**769**-617-*599-447*	Pentagalloylhexose [abj]
51	10.3	275	1085	**783**-633-451-*301*	HHDP-galloyltergalloylhexose (1) [ad]
52	10.5	260	933	631-481-**451**-*301*	HHDP-tergalloylhexose (6) [adefj]
53	10.5	260	1083(Nf), 541[M-2H]²⁻	[541]: 631-466-451-301	Ditergalloylhexose (trace) (1) [d]
54	10.7	350	447	**301**-*255--217-207-179-151*	Quercetin deoxyhexoside (quercetin-3-rhamnoside[b]) [ahij]
55	10.8	260	1087	935-**917**-749-451	Di-HHDP-digalloylhexose
56	10.9	260	1083(Nf), 541[M-2H]²⁻	[541]: 631-452-*301*	Ditergalloylhexose (trace) (2) [d]
57	12.2	260	1085	**783**-633-*481-451-301*	HHDP-galloyltergalloylhexose (2) [ad]
58	13.3	366	301	*179-151*	Quercetin [i]

*Ionization in negative mode for all compounds except for anthocyanins in positive mode. The main fragment in MS^2 is given in boldface, the minor fragments are given in normal font and the ultra-minor fragments are given in italics. HHDP: hexahydroxydiphenoyl group. Std: identified with authentic standard. Nf: not fragmented. [M-2H]$^{2-}$: doubly charged ion.

[a]Quatrin et al., 2019; [b]Plaza et al., 2016; [c]Fischer et al., 2011; [d]Garcia-Villalba et al., 2015; [e]Pereira et al., 2017; [f]Fracassetti et al., 2013; [g]Tavares et al., 2016; [h]Wu et al., 2012; [i]Neves et al., 2018; [j]Albuquerque et al., 2020; [k]Morales et al., 2016.

Table 2. Contents in various phenolic classes for dried jabuticaba peel after extraction by ultrasound technology and conventional solvent extraction.

	Gallic acid derivatives (mg/g DJP)	Ellagic acid (mg/g DJP)	Flavonol derivatives (mg/g DJP)	Anthocyanin derivatives (mg/g DJP)	Sum of phenolic compounds (mg/g DJP)
Ultrasound extraction	9.23 ± 0.32 (a)	1.08 ± 0.02 (a)	0.24 ± 0.01 (b)	7.81 ± 0.06 (b)	18.36 ± 0.36 (a)
Solvent extraction	4.89 ± 0.65 (b)	1.11 ± 0.07 (a)	0.32 ± 0.02 (a)	10.22 ± 1.17 (a)	16.53 ± 1.19 (a)

Values represent mean ± SD (n = 3). Sum of phenolic compounds is obtained from the different columns on the left (UPLC). DJP: dried jabuticaba peel; Different letters indicate a significant difference between both extracts at $p < 0.05$.

Table 3. Acid hydrolysis of dried jabuticaba peel and DJP extract obtained after ultrasound extraction followed by UPLC/DAD/ESI-MS[n] analysis of phenolic compounds.

N°	RT (min)	λ$_{max}$ (nm)	[M - H]⁻ (m/z)	MS² fragments (m/z)	Tentative identification	DJP (mg/g DJP)			US extract (mg/g DJP)		
						Supernatant	Pellet	Sum	Supernatant	Pellet	Sum
1	1.2	271	169	125	Gallic acid (Std) [ab]	10.7 ± 0.3	0.75 ± 0.02	11.4 ± 0.3	6.27 ± 0.73	0.02 ± 0.01	6.29 ± 0.74
2	1.35	281	483	**331**-313-169	Digalloylhexose [ab]	0.95 ± 0.23	-	0.95 ± 0.23	0.89 ± 0.03	-	0.89 ± 0.03
3	2.2	284	313	*295-245-169-125-107*	Gallic acid *C*-hexoside (dehydrated form) [c]	26.9 ± 4.6	3.49 ± 0.09	30.4 ± 3.8	18.6 ± 1.5	0.77 ± 0.34	19.4 ± 1.8
4	2.55	276	181	**137**-*109*	DiOH-phenylpropionic acid [d]	5.07 ± 0.72	-	5.07 ± 0.72	0.67 ± 0.18	-	0.67 ± 0.18
5	3.6	374	783	**481**-451-*301*-299-271	HHDP-ellagic acid-*C*-hexoside (1)	0.12 ± 0.04	-	0.12 ± 0.04	0.13 ± 0.04	-	0.13 ± 0.04
6	3.85	375	783	**481**-451-*301*-299-271	HHDP-ellagic acid-*C*-hexoside (2)	0.45 ± 0.07	-	0.45 ± 0.07	0.32 ± 0.05	-	0.32 ± 0.05

#	RT			Fragments	Identification						
7	4.4	365	631	**451**-407-299-271	Valoneic/sanguisorbic acid dilactone C-hexoside or Tergalloyl-C-hexose (1) [b]	-	-	-	-	-	-
8	4.6	365	783	**481**-451-301-299-271	HHDP-ellagic acid-C-hexoside (3)	-	-	-	-	-	-
9	4.65	365	631	587-451-301-**299**-271	Valoneic/sanguisorbic acid dilactone C-hexoside or Tergalloyl-C-hexose (2) [b]	-	-	-	-	-	-
10	4.7	365	783	767-**483**-453-303-271	HHDP-ellagic acid-C-hexoside (4)	-	-	-	-	-	-
11	4.75	365	631	451-301-**299**-271	Valoneic/sanguisorbic acid dilactone C-hexoside or Tergalloyl-C-hexose (3) [b]	-	-	-	-	-	-
12	5	365	631	587-451-**299**-271	Valoneic/sanguisorbic acid dilactone C-hexoside or Tergalloyl-C-hexose (4) [b]	-	-	-	-	-	-
13	5.1	365	631	587-451-301-**299**-271	Valoneic/sanguisorbic acid dilactone C-hexoside or Tergalloyl-C-hexose (5) [b]	-	-	-	-	-	-
14	5.9	370	469	451-**425**-407-301-167	Valoneic acid dilactone [be]	0.73 ± 0.06	3.44 ± 0.09	4.17 ± 0.09	0.99 ± 0.07	2.02 ± 0.10	3.02 ± 0.17
15	6.15	365	469	*451*-**425**-301-299	Sanguisorbic acid dilactone [be]	-	1.39 ± 0.04	1.39 ± 0.04	-	0.85 ± 0.04	0.85 ± 0.04
16	8.4	367	301	*258-229-186*	Ellagic acid (Std) [abf]	3.52 ± 0.14	12.9 ± 0.5	16.4 ± 0.4	3.62 ± 0.38	7.24 ± 0.61	10.9 ± 1.0
TOTAL PHENOLIC COMPOUNDS						48.4 ± 4.1	21.9 ± 0.9	70.3 ± 3.2	31.5 ± 1.3	10.9 ± 0.5	42.4 ± 1.6

The main fragment in MS^2 is given in boldface, the minor fragments are given in normal font and the ultra-minor fragments are given in italics. Values represent mean ± SD (n = 3). Sum of phenolic compounds is the addition of Supernatant and Pellet. Std: identified with authentic standard. −: Means below quantification limit or not present.

[a]Quatrin et al., 2019; [b]Garcia-Villalba et al., 2015; [c]Fischer et al., 2011; [d]Fragmentation as for standard; [e]Morales et al., 2016; [f]Neves et al., 2018.